3D Neutronic and Secondary Particles Analysis on YBa$_{2}$Cu$_{3}$O$_{7-\delta }$ Tapes for Compact Fusion Reactors

3D neutronic and secondary particles analysis on $YBa_2Cu_3O_{7-\delta}$ tapes for compact fusion reactors

Federico Ledda*, Daniele Torsello*, Davide Pettinari, Simone Sparacio, Zachary Hartwig, Massimo Zucchetti, Francesco Laviano

***Abstract*—The development of compact fusion reactors relies on high temperature superconductors to generate the required high field. In this frame Rare-Earth Barium Copper Oxide tapes appear as the most promising solution. However, these tapes will experience a radiation harsh environment due to the high flux and fluence of energetic neutrons and of the secondary particles produced by the neutrons interaction with the materials. Realistic 3D Monte Carlo simulations represent the required tool to reliably estimate the radiation environment of the tapes, providing the starting point for experimental investigation of their radiation hardness and performance under working conditions. In this paper a comprehensive analysis of damage and energy deposition including secondary particles on a 3D model of a VIPER cable is carried out, starting from a 3D model of an ARC-class reactor.**

***Index Terms*—HTS radiation hardness. Compact fusion reactors.**

I. Introduction

COMPACT fusion reactor concepts rely on high magnetic fields for effective plasma confinement, making High Temperature Superconducting (HTS) magnets an enabling technology [1]. In the design effort aimed to the overall size reduction, great importance was devoted to guarantee that tritium breeding and power deposition were sufficient for power plants operation, leaving radiation damage issues in the background. However, radiation damage is a critical issue for the assessment of magnets lifetime and performances during operations, and the compact size gives even more importance to the evaluation of the neutron spectrum and flux at the magnet position [2]. A trade off analysis between these parameters with high fidelity neutronics constitutes a fundamental step for an effective reactor project. Furthermore, neutron interactions with all the materials in the reactor produce secondary particles (i.e., ions, electrons, photons, etc.) that, if generated close enough to the HTS, can contribute to magnet irradiation damage. The contribution from these particles to the overall damage has been neglected so far, but their interaction with the superconductor might produce a non negligible localized damage that is worth investigating. In the present work, we consider a 3D model of an ARC-class reactor to carry out a neutronic and secondary particle analysis, considering radiation damage and thermal deposition. Neutron spectrum and flux have been evaluated at the Toroidal Field magnets position using the Monte Carlo (MC) Particle and Heavy Ion Transport code System PHITS [3]. Starting from the calculated spectrum in the most critical position, a more refined analysis including secondary particles was performed on a 3D model of an HTS based VIPER cable [4] within PHITS, resulting in an estimate of the secondary particle spectra in the HTS. The importance of dedicated neutron shielding was also considered. The inventory code Fispact-II [5] was then employed to preliminarily assess the impact of the decay heat of the HTS stack when compared with the power deposited by neutrons.

This work is partially supported by the Ministry of Education, Universities and Research through the "Programma Operativo Nazionale (PON) Ricerca e Innovazione 2014–2020", and through the National Recovery and Resilience Plan funded by the European Union- NextGenerationEU, by the European Cooperation in Science and Technology (COST) action CA19108: "High-Temperature Superconductivity for Accelerating the Energy Transition", by the Italian Ministry of Foreign Affairs and International Cooperation, grant number US23GR16, and by Eni S.p.A.. Support from CINECA for high-performance computing is also acknowledged.

F. Ledda, S. Sparacio, F. Laviano, D. Torsello are with the Department of Applied Science and Technology, Politecnico di Torino, and INFN - Sez. Torino, Torino, Italy (e-mail: daniele.torsello@polito.it).

D. Pettinari, M. Zucchetti are with the Department of Energy, Politecnico di Torino, Italy

Z. Hartwig is with the MIT Plasma Science and Fusion Center, United States of America.

*These authors contributed equally.

II. Modelling

A. Monte Carlo code

MC codes represent one of the basic tools in nuclear system design, being widely exploited to evaluate neutron distribution and irradiation-related quantities in basically all the relevant applications, from research to radiation therapy [6], [7]. Many MC codes have been developed [3], [8]–[11]. In the present paper, the software PHITS was employed because it allows to transport and collide nearly all particles over a large energy range, to import CAD based geometries using tetrahedral meshes to define the domain without the use of the classical Constructive Solid Geometry procedure, and because it supports parallelization schemes needed to perform onerous calculations on High Performances Computers [3]. PHITS is able to evaluate displacement-per-atom (dpa) with a 3 steps procedure: transport calculation including nuclear interaction, calculation of Coulomb elastic scattering cross-section between incident charged particle or Primary Knock-on atoms (PKAs) and the target atom and cascade damage approximation [12]. Thanks to the implemented Event Generation Mode, PHITS can produce PKAs while preserving energy and momentum conservation in a reaction using the nuclear data library [12]. Japanese Evaluated Nuclear Data Library (JENDL-4.0) [13] in the compact ENDF (ACE) format constitutes the native nuclear data library in PHITS, but any dataset in this format can be chosen. JENDL-4.0 was considered the reference in this work, but Evaluated Nuclear Data

File (ENDF/B-VIII.0) and Fusion Evaluated Nuclear Data Library (FENDL-3.2) libraries were also used and confirmed the reported results. A comprehensive comparison of PHITS with OpenMC [10] for the radiation environment of compact tokamaks has been carried out elsewhere [14], and results from PHITS were also compared with the Monte Carlo N-Particles (MCNP) code for fusion applications [15].

PHITS can also be used to directly evaluate radiation damage with the dpa-tally, adopting the NRT-dpa formulation [3], [5], [12], neglecting athermal recombination and considering a defect generation efficiency equal to 0.8. The displacement energy thresholds were se to the default values: 25 eV for Y, Ba and O, and 40 eV for Cu [12], [16].

Finally, nuclear power deposition is another quantity that can be extracted from a MC simulation. It represents a fundamental parameter for magnet design and engineering, constituting a volumetric heat source on the system itself. The overall power deposition (due to both neutrons and secondary particles) can be computed in PHITS which tallies each subdomain of the simulation.

For all the simulations, the lower cutoff energy for secondary particles (electrons, photons and protons) was set at 1 keV, i.e. the minimum energy allowed in PHITS for this parameter.

B. ARC model

Given the lack of a definitive design for the magnetic system in the next generation compact tokamaks, a two-steps workflow has been followed to analyze the superconducting cable. This procedure also allowed a reduction of the computational cost with respect to performing a MC simulation on a complete reactor (including small elements such as HTS tapes) with acceptable errors, and to obtain results with a broad applicability. Firstly, a model of the inner components of ARC was built by the authors following the design reported in [1], [17]: a D-shaped plasma chamber, composed of a W first wall, a Be neutron multiplier layer, and an Inconel-718 vacuum vessel submerged in a FLiBe tank [1], [17], [18]. Note that this is the basic design, in which no material dedicated only to neutron shielding was yet included (several options are currently being evaluated [18], [19]). The described design has been originally realized on SolidWorks®, and imported in the MC code after the generation of an appropriate tetrahedral mesh on COMSOL Multiphysics® [20].

To save computational resources, simulations have been performed on a reduced 10 degrees domain with reflective boundary conditions on the cut faces, to reconstruct an equivalent model of the whole reactor. A neutron source reproducing the shape of the plasma in a tokamak was coded and introduced in PHITS, considering the expected spatial and energy distribution of neutron emission into a magnetically confined D-T plasma [14], [21]. The emissivity of the source was evaluated on the basis of the plasma power [1] in 1.8×10^{20} n/s. The neutron flux outgoing from the vacuum vessel of this model at the most critical point (point A of fig. 1 [14]), was then employed as a source for the second step, i.e. the simulations on an HTS cable. Point A identifies the external surface of the FLiBe chamber, i.e. the boundary between the inner part of the reactor and the region where the magnet system will be. This region is the closest to the plasma that will be occupied by the magnetic system, and therefore the most exposed to the radiation load. The neutron spectrum at point A was implemented for the second step as a planar source, emitting collimated neutrons toward the HTS cable. Although a detailed neutron shielding design is outside the scope of this work, we also implemented a simple shielding solution (following [18] and [19]), by adding a 50 cm thick ZrH_2 layer between the planar source and the HTS cable.

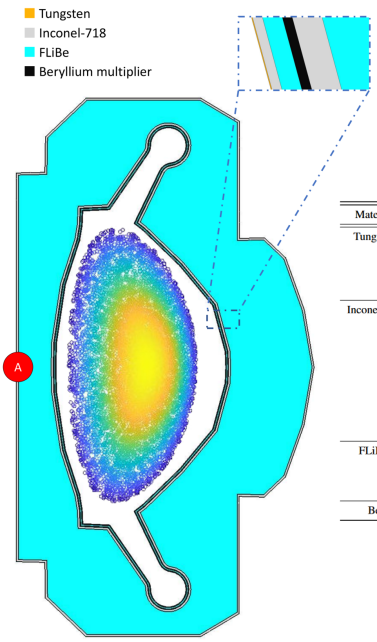

Material	Element	Mass fraction (%)	Density (g/cm^3)
Tungsten	^{180}W	0.12	19.25
	^{182}W	26.5	
	^{183}W	14.31	
	^{184}W	30.64	
	^{186}W	28.43	
Inconel-718	Al	0.52	8.19
	C	0.021	
	Co	0.11	
	Cr	19.06	
	Cu	0.02	
	Fe	18.15	
	Mo	3.04	
	Ti	0.93	
	Nb	5.08	
	Ni	53	
FLiBE	F	0.57	1.94
	Be	0.14	
	^{6}Li	0.26	
	^{7}Li	0.03	
Be	^{9}Be	100	1.85

Fig. 1. The ARC model and the source employed in the simulations. The location in which the neutron spectrum used as input for the cable simulation was evaluated is indicated by the point A. The table shows the composition of each material.

C. VIPER model

The calculations were carried out on the VIPER cable design, which was developed in particular for compact fusion reactors [4]. Geometrically, the VIPER cable consists in a cylindrical copper core with rectangular channels (twisted along the length of the cable) on the perimeter designed to fit stacks of HTS tapes impregnated with a solder. A cryogenic coolant (He in the present work) flows through a central channel, while a copper matrix is surrounded in a stainless steel external jacket. REBCO is used in the HTS tapes as superconducting material [4].

A one-pitch 3D model was built on COMSOL Multiphysics® [20] and imported in PHITS thanks to the CAD-import utility (a cross section is shown in fig. 2). The material composition adopted for the model is shown in Table I and the stack details are based on the specifications of SuperPower® tapes [22]. Natural isotopic composition was assumed for elements in materials.

TABLE I
MATERIAL COMPOSITION IN THE VIPER MODEL.

Component	Atomic mass fraction [%]														
	Fe	Cr	Ni	Pb	Sn	Mo	W	Mn	Co	Cu	N	Ag	Y	Ba	O
Solder	.	-	-	70	30	-	-	-	-	-	-	-	-	-	-
Internal jacket	-	-	-	-	-	-	-	-	-	100	-	-	-	-	-
Copper matrix	-	-	-	-	-	-	-	-	-	100	-	-	-	-	-
External jacket	71.9	16	10	-	-	2	-	-	-	-	0.1	-	-	-	-
HTS stack	2.08	8.08	29.7	-	-	8.86	1.56	0.52	1.3	42.32	-	4.73	0.16	0.49	0.2

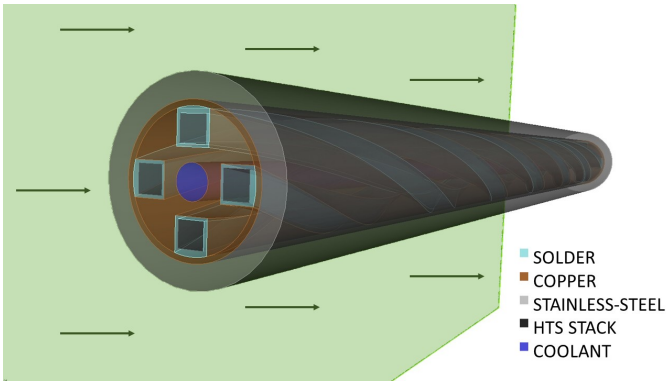

Fig. 2. The VIPER model and the neutron planar source employed in the PHITS code.

D. FISPACT

In addition to the effect of lattice damage by atomic displacement [23], neutrons also undergo nuclear reactions with the target materials. As a consequence of neutron capture, nuclei enter in an excited, unstable state, from which they come out emitting energy in the form of radiation [24]. The induced radioactivity can constitute an issue for component decommissioning [25] and the decay heat sums up to the one deposited by the neutron flux. An estimation of the relevance of this power fraction during the operation life-time of reactors can be useful, also considering the enhanced neutron flux experienced in compact tokamaks. The inventory software Fispact-II [5] was employed for this aim.

III. RESULTS AND DISCUSSION

A. Heat deposition

Fig. 3 shows the total power deposition computed on each subdomain of the cable. As can be noted the most sensitive element in the cable, the HTS stack, is also the most heated per unit volume, with about 117 kW/m^3. This is due to the material composition of the stack, including a not negligible amount of Ni, prone to nuclear reactions. A detailed analysis of the thermal and electromagnetic behaviour of the VIPER cable under this regime of irradiation has been carried out in [26]. Furthermore, a preliminary activation analysis of the HTS stack was carried out with Fispact-II, to verify whether the heat generated in HTS components activated by the fusion radiation environment could play a role in the performance of the superconducting cable. According to our evaluation, this fraction of power is negligible when compared with the fraction deposited directly by neutrons on the magnetic system since even after 10 years of operation it will be 5 orders of magnitude smaller. A complete activation analysis for superconducting components will be proposed in a forthcoming paper.

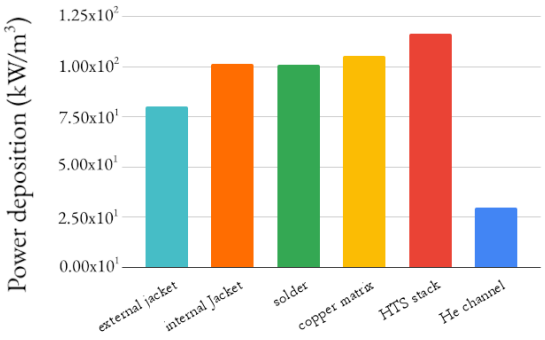

Fig. 3. Volumetric heat deposition due to neutron irradiation on different component of the superconducting cable, without shield.

B. Energetic particles environment

The neutron spectrum on the HTS stack is shown in fig. 4, compared with the neutron spectrum at point A of fig. 1; the ratio between them was also evaluated to point out spectral shifts and it is shown in the lower panel.

Considering the unshielded case, for energies higher than about 5 MeV, the source neutron spectrum appears to be higher, while an increase of the flux on the stack is found for lower energies. Considering the reduced size of the cable and the small total amount of neutrons in the more energetic groups (i.e. in the energy range between 3.6 MeV and 14.1 MeV) with respect to the slow tail, this increase can not be ascribed to particle thermalization only (that is responsible for most of the spectral shift from high energies to low energies). Therefore, we attribute an important contribution in this direction to inelastic (n,Xn) reactions. In fact, the total neutron flux increases from $7.7 \times 10^{12} \pm 2 \times 10^{11}$ $n/cm^2 s$ to $1.127 \times 10^{13} \pm 1 \times 10^{10}$ $n/cm^2 s$ when considering the source and the HTS stack, respectively. Given the small volumes of VIPER subdomains (HTS stacks, jackets, solders, etc) with respect to the mean free path of neutrons, no information about the origin of such a multiplication can be obtained by a simple comparison of spectra on different regions. However, PHITS provides also the medium-wise total number of n-collisions

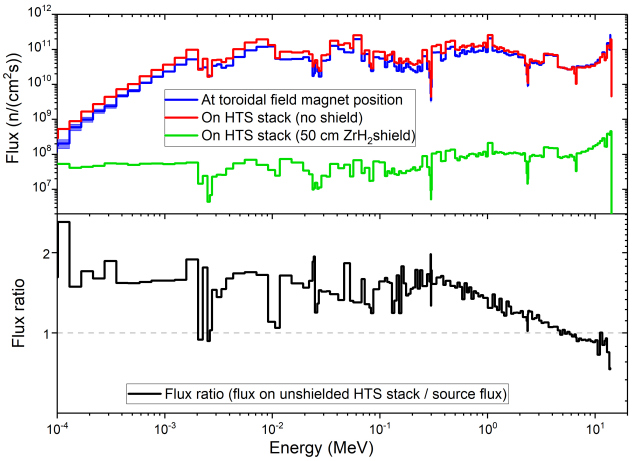

Fig. 4. Upper panel: neutron spectra impinging in the most critical point of the toroidal field magnet (point A of fig. 1 - blue line), and evaluated on the HTS stack without (red line) and with (green line) the neutron shield. Lower panel: ratio between the neutron spectra computed on the HTS stack (unshielded) and at point A.

(the average number of n-collisions in each material of the model) per source and region. It shows a predominance of capture reactions in stainless-steel and in the copper matrix, with a comparable frequency of n-Xn reaction rates in all the materials. An analogous result is provided for inelastic collisions in the high energy range. A possible approach to identify the origin of the neutron population increment is evaluating multiplication cross sections for the main elements composing the system. The stainless steel of the external jacket mainly consist in Fe, Ni and Cr; Pb and Sn are employed in the solder, while the HTS stack is made of Cu and Ni for the majority. Copper is used in the internal matrix and jacket as well. Considering their most abundant isotopes in natural composition, an appreciable n-2n cross section (larger than 100 mb) is present for incident neutron energy higher than 11 MeV (higher than 7 MeV for Pb208 and Sn) [27]. This hypothesis was also verified performing a PATHWAY analysis in FISPACT-II. The introduction of the ZrH_2 layer, on the other hand, strongly reduces the flux of neutrons on the cable, with a considerable thermalizing effect. In particular, the total flux computed on the HTS stack is $3.9110 \times 10^{10} \pm 9 \times 10^{6}$ n/cm^2s, with an abatement of about 3 orders of magnitude.

Exploiting the capability of PHITS of transporting also photons and charged particles [3], photons, electrons and protons spectra outgoing from ARC have been evaluated, as well as those generated in the cable (see fig. 5). The similarity between the electron spectra is due to the local nature of this radiation and to the similar abundance of elements in the reactor and in the cable (i.e. Ni, Cu, Fe and Cr), and analogous considerations can be made for protons [28]. Therefore, the secondary radiation is relevant only on a short distance (cm to μm for photons and charged particles, respectively), producing local effects. The fraction produced in the vacuum vessel will not be deposited directly on the superconducting system, being shielded by the cryostats. The introduction of a shielding layer has a considerable impact also on the secondary particle emission, modifying the spectra according to a moderated neutron flux and producing an overall reduction of the total fluxes of several order of magnitude. The dpa induced by these secondary particles is already taken into account by PHITS and contributes to the total damage discussed below. However, it should be noted that the impact of these fluxes of energetic particles might affect the operation of the HTS [29], since they could induce a local suppression of superfluid density, and their effect is yet to be fully determined, also experimentally.

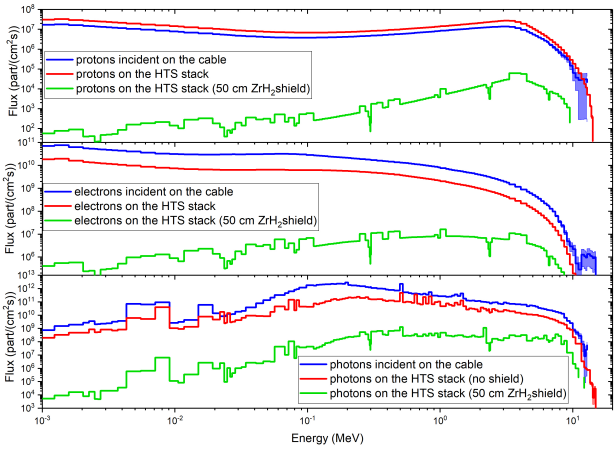

Fig. 5. Secondary particle spectra on the superconducting stack without shielding (red lines) and with a 50 cm thick shielding layer (green lines), compared with ARC-outgoing ones at point A of fig. 1 (blue lines). Protons are shown in the upper panel, electrons in the middle panel and photons in the lower panel.

C. Radiation damage

Radiation damage was evaluated on the superconducting material (by simulations on the VIPER cable in which the stack was considered as composed of pure YBCO) using the default library (JENDL-4.0), as well as the FENDL-3.2 and ENDF/B-VIII.0 datasets for the unshielded case, and with the JENDL-4,0 library when the neutron shield is added, as presented in Table II.

TABLE II
DISPLACEMENT PER ATOM (DPA) EVALUATED DIRECTLY FROM THE PHITS CODE, CONSIDERING 3 DIFFERENT NUCLEAR LIBRARIES AND THE IMPACT OF A NEUTRON SHIELD.

Code	shielding	dpa after 10 years	time to 4mdpa
PHITS ENDF/B-VIII.0	no	9.70×10^{-1}	15 days
PHITS FENDL-3.2	no	9.90×10^{-1}	15 days
PHITS JENDL-4.0	no	9.86×10^{-1}	15 days
PHITS JENDL-4.0	50 cm	3.11×10^{-3}	12.8 years

The lattice damage after 10 years of full-power irradiation without any shielding is evaluated in 0.99 dpa employing the JENDL-4.0 library and 0,90 and 0.97 dpa employing the FENDL-3.2 and the ENDF/B-VIII.0 neutron data sets.
The three results corroborate the order of magnitude of a previous estimate based on rougher approximations, confirming that suitable radiation shields will be essential [2]. The

difference with the previous finding could be mainly ascribed to the introduction of the realistic 3D geometry, in this work, and secondly to different assumptions on neutrons emission intensity from the plasma (assumed being equal to 1.8×10^{20} n/s and 2×10^{20} n/s in the present paper and in the previous estimate, respectively). The introduction of the ZrH_2 layer is able to mitigate the radiation damage, leading to the value of 3.11×10^{-3} dpa after 10 FPY. The time needed to accumulate a damage equal to 4 mdpa under this radiation regime is also presented, considering that this value was found as a reference limit at which REBCO ability to carry current starts to fall below its initial value [29], [30].

IV. Conclusions

In summary, a comprehensive 3D MC transport analysis on a superconducting VIPER cable was carried out, evaluating both neutron and secondary particles spectra. Radiation damage on the HTS stack was evaluated at the most exposed part of the toroidal field magnet in an ARC-class reactor without shielding, yielding the value of 0.95 $\pm$ 0.04 dpa in 10 years of full power irradiation. This finding supports and refines previous estimations, stressing the necessity of a suitable shielding layer for the magnet system. A simple neutron shielding solution was here considered and, although being able to eventually extend the lifetime of the HTS magnet above 10 FPY, it corresponds to an increase the diameter of the reactor of about 1 m. Therefore, the magnet design will be also strongly affected. A careful neutron shielding design and its impact on all the reactor components is thus required. Finally, we estimate the volumetric heat deposition by neutrons in the HTS stack and we find a negligible role of the heat generated in the materials by activation, even after ten years of operation.

References

[1] B. Sorbom, J. Ball, T. Palmer, F. Mangiarotti, J. Sierchio, P. Bonoli, C. Kasten, D. Sutherland, H. Barnard, C. Haakonsen *et al.*, "Arc: a compact, high-field, fusion nuclear science facility and demonstration power plant with demountable magnets," *Fusion Engineering and Design*, vol. 100, pp. 378–405, 2015.

[2] D. Torsello, D. Gambino, L. Gozzelino, A. Trotta, and F. Laviano, "Expected radiation environment and damage for ybco tapes in compact fusion reactors," *Superconductor Science and Technology*, vol. 36, no. 1, p. 014003, dec 2022. [Online]. Available: https://dx.doi.org/10.1088/1361-6668/aca369

[3] Y. Iwamoto, T. Sato, S. Hashimoto, T. Ogawa, T. Furuta, S. ichiro Abe, T. Kai, N. Matsuda, R. Hosoyamada, and K. Niita, "Benchmark study of the recent version of the phits code," *Journal of Nuclear Science and Technology*, vol. 54, no. 5, pp. 617–635, 2017. [Online]. Available: https://doi.org/10.1080/00223131.2017.1297742

[4] Z. S. Hartwig, R. F. Vieira, B. N. Sorbom, R. A. Badcock, M. Bajko, W. K. Beck, B. Castaldo, C. L. Craighill, M. Davies, J. Estrada, V. Fry, T. Golfinopoulos, A. E. Hubbard, J. H. Irby, S. Kuznetsov, C. J. Lammi, P. C. Michael, T. Mouratidis, R. A. Murray, A. T. Pfeiffer, S. Z. Pierson, A. Radovinsky, M. D. Rowell, E. E. Salazar, M. Segal, P. W. Stahle, M. Takayasu, T. L. Toland, and L. Zhou, "Viper: an industrially scalable high-current high-temperature superconductor cable," *Superconductor Science and Technology*, vol. 33, no. 11, p. 11LT01, oct 2020. [Online]. Available: https://dx.doi.org/10.1088/1361-6668/abb8c0

[5] M. g. Michael Fleming, Thomas Stainer, *the Fispact-II User Manual*, 2018.

[6] A. M. Sukegawa, H. Kawasaki, K. Okuno *et al.*, "Conceptual radiation shielding design of superconducting tokamak fusion device by phits," *Prog. Nucl. Sci. Technol.*, vol. 2, pp. 375–381, 2011.

[7] H. Horiguchi, T. Sato, H. Kumada, T. Yamamoto, and T. Sakae, "Estimation of relative biological effectiveness for boron neutron capture therapy using the PHITS code coupled with a microdosimetric kinetic model," *Journal of Radiation Research*, vol. 56, no. 2, pp. 382–390, 11 2014. [Online]. Available: https://doi.org/10.1093/jrr/rru109

[8] J. Leppänen, M. Pusa, T. Viitanen, V. Valtavirta, and T. Kaltiaisenaho, "The serpent monte carlo code: Status, development and applications in 2013," *Annals of Nuclear Energy*, vol. 82, pp. 142–150, 2015, joint International Conference on Supercomputing in Nuclear Applications and Monte Carlo 2013, SNA + MC 2013. Pluri- and Trans-disciplinarity, Towards New Modeling and Numerical Simulation Paradigms. [Online]. Available: https://www.sciencedirect.com/science/article/pii/S0306454914004095

[9] T. Goorley, M. James, T. Booth, F. Brown, J. Bull, L. J. Cox, J. Durkee, J. Elson, M. Fensin, R. A. Forster, J. Hendricks, H. G. Hughes, R. Johns, B. Kiedrowski, R. Martz, S. Mashnik, G. McKinney, D. Pelowitz, R. Prael, J. Sweezy, L. Waters, T. Wilcox, and T. Zukaitis, "Initial mcnp6 release overview," *Nuclear Technology*, vol. 180, no. 3, pp. 298–315, 2012. [Online]. Available: https://doi.org/10.13182/NT11-135

[10] P. K. Romano and B. Forget, "The openmc monte carlo particle transport code," *Annals of Nuclear Energy*, vol. 51, pp. 274–281, 2013. [Online]. Available: https://www.sciencedirect.com/science/article/pii/S0306454912003283

[11] F. Tabbakh, "Particles transportation and nuclear heating in a tokamak by mcnpx and geant4," *Journal of Fusion Energy*, vol. 35, no. 2, pp. 401–406, 2016.

[12] Y. Iwamoto, S. ichiro Meigo, and S. Hashimoto, "Estimation of reliable displacements-per-atom based on athermal-recombination-corrected model in radiation environments at nuclear fission, fusion, and accelerator facilities," *Journal of Nuclear Materials*, vol. 538, p. 152261, 2020. [Online]. Available: https://www.sciencedirect.com/science/article/pii/S0022311520304670

[13] K. SHIBATA, O. IWAMOTO, T. NAKAGAWA, N. IWAMOTO, A. ICHIHARA, S. KUNIEDA, S. CHIBA, K. FURUTAKA, N. OTUKA, T. OHSAWA, T. MURATA, H. MATSUNOBU, A. ZUKERAN, S. KAMADA, and J. ichi KATAKURA, "Jendl-4.0: A new library for nuclear science and engineering," *Journal of Nuclear Science and Technology*, vol. 48, no. 1, pp. 1–30, 2011. [Online]. Available: https://doi.org/10.1080/18811248.2011.9711675

[14] F. Ledda and et al, "3d neutronic analysis on compact fusion reactors: Phits-openmc cross-comparison," *submitted*, vol. x, no. Y, p. Z, 2023.

[15] A. M. Sukegawa, K. Takiyoshi, T. Amano, H. Kawasaki, and K. Okuno, "Neutronic analysis of fusion tokamak devices by phits," *Prog. Nucl. Sci. Technol*, vol. 1, pp. 36–39, 2011.

[16] M. Norgett, M. Robinson, and I. Torrens, "A proposed method of calculating displacement dose rates," *Nuclear Engineering and Design*, vol. 33, no. 1, pp. 50–54, 1975. [Online]. Available: https://www.sciencedirect.com/science/article/pii/0029549375900357

[17] A. Kuang, N. Cao, A. Creely, C. Dennett, J. Hecla, B. LaBombard, R. Tinguely, E. Tolman, H. Hoffman, M. Major, J. Ruiz Ruiz, D. Brunner, P. Grover, C. Laughman, B. Sorbom, and D. Whyte, "Conceptual design study for heat exhaust management in the arc fusion pilot plant," *Fusion Engineering and Design*, vol. 137, pp. 221–242, 2018. [Online]. Available: https://www.sciencedirect.com/science/article/pii/S0920379618306185

[18] S. Segantin, S. Meschini, R. Testoni, and M. Zucchetti, "Preliminary investigation of neutron shielding compounds for arc-class tokamaks," *Fusion Engineering and Design*, vol. 185, p. 113335, 2022.

[19] J. W. Bae, E. Peterson, and J. Shimwell, "Arc reactor neutronics multi-code validation," *Nuclear Fusion*, 2022.

[20] "Comsol: Multiphysics software for optimizing designs," 2023, accessed Jul.05, 2023.

[21] C. Fausser, A. L. Puma, F. Gabriel, and R. Villari, "Tokamak d-t neutron source models for different plasma physics confinement modes," *Fusion Engineering and Design*, vol. 87, no. 5, pp. 787–792, 2012, tenth International Symposium on Fusion Nuclear Technology (ISFNT-10). [Online]. Available: https://www.sciencedirect.com/science/article/pii/S0920379612000853

[22] "Superpower inc." accessed Jul. 2023. [Online]. Available: https://www.superpower-inc.com/specification.aspx

[23] K. Nordlund, S. J. Zinkle, A. E. Sand, F. Granberg, R. S. Averback, R. E. Stoller, T. Suzudo, L. Malerba, F. Banhart, W. J. Weber, F. Willaime, S. L. Dudarev, and D. Simeone, "Primary radiation damage: A review of current understanding and models," *Journal of Nuclear Materials*, vol. 512, pp. 450–479, 2018. [Online]. Available: https://www.sciencedirect.com/science/article/pii/S002231151831016X

[24] M. F.L'annunziata, *Handbook of radioactivity analysis*. Academic Press,Elsevier, 2012.

[25] M. Zucchetti, "Improvements of net/iter shielding to limit short-term radioactivity in magnet materials," *Fusion Engineering and Design*, vol. 18, pp. 349–354, 1991. [Online]. Available: https://www.sciencedirect.com/science/article/pii/092037969190150O

[26] S. Sparacio and et al, "Analysis of thermal effects of plasma operation on hts-based tf-coil conductors," *submitted*, vol. x, no. Y, p. Z, 2023.

[27] "Java based nuclear information software janis- nuclear energy agency," accessed Aug.2023. [Online]. Available: https://www.oecd-nea.org/jcms/pl_39910/janis

[28] G.W.Morgan, "Some practical considerations in radiation shielding,isotopes division circular b-4," *U.S. Atomic Energy Commission, Oak Ridge*, 1949.

[29] W. Iliffe, K. Adams, N. Peng, G. Brittles, R. Bateman, A. Reilly, C. Grovenor, and S. Speller, "The effect of in situ irradiation on the superconducting performance of reba2cu3o7- δ-coated conductors," *MRS Bulletin*, pp. 1–10, 2023.

[30] D. X. Fischer, R. Prokopec, J. Emhofer, and M. Eisterer, "The effect of fast neutron irradiation on the superconducting properties of rebco coated conductors with and without artificial pinning centers," *Superconductor Science and Technology*, vol. 31, no. 4, p. 044006, mar 2018. [Online]. Available: https://dx.doi.org/10.1088/1361-6668/aaadf2